Accepted Manuscript

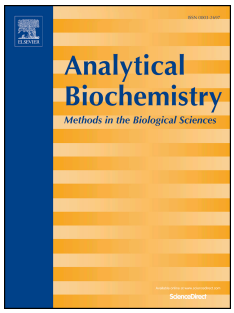

Split luciferase-based biosensors for characterizing EED binders

Ling Li, Lijian Feng, Minlong Shi, Jue Zeng, Zijun Chen, Li Zhong, Li Huang, Weihui Guo, Ying Huang, Wei Qi, Chris Lu, En Li, Kehao Zhao, Justin Gu

PII: S0003-2697(17)30036-2

DOI: 10.1016/j.ab.2017.01.014

Reference: YABIO 12607

To appear in: *Analytical Biochemistry*

Received Date: 2 November 2016

Revised Date: 13 January 2017

Accepted Date: 18 January 2017

Please cite this article as: L. Li, L. Feng, M. Shi, J. Zeng, Z. Chen, L. Zhong, L. Huang, W. Guo, Y. Huang, W. Qi, C. Lu, E. Li, K. Zhao, J. Gu, Split luciferase-based biosensors for characterizing EED binders, *Analytical Biochemistry* (2017), doi: 10.1016/j.ab.2017.01.014.

Split luciferase-based biosensors for characterizing EED binders

Ling Li[1*], Lijian Feng[1], Minlong Shi[1], Jue Zeng[1], Zijun Chen, Li Zhong, Li Huang, Weihui Guo, Ying Huang, Wei Qi, Chris Lu, En Li, Kehao Zhao, Justin Gu[*]

[1] These authors contributed equally to this study

[*] Corresponding authors：

Justin Gu (Justin.gu@novartis.com) and Ling Li (ling-1.li@novartis.com)

China Novartis Institutes for Biomedical Research, 4218 Jinke Road, Shanghai 201203, China

Abbreviations:

EED, embryonic ectoderm development; PRC2, polycomb repressive complex 2; DSF, differential scanning fluorimetry; ITC, isothermal titration calorimetry; EZH2, enhancer of zeste homolog 2; SUZ12, suppressor of zeste 12; SAM, S-Adenosyl methionine; EEDi, EED inhibitor; SRM, stimulation responsive motif; ELISA, enzyme-linked immunosorbent assay; SAR, structure-activity relationship; wt, wild type; luc, luciferase; N-Luc, N-terminal domain of luciferase; C-Luc, C-terminal domain of luciferase; EBD, EED binding domain (EZH2 residue 40-68); AEBP2, adipocyte enhancer-binding protein 2; RbAp48, retinoblastoma binding protein 48; SAH, S-Adenosyl homocysteine; LC, liquid chromatography; MS, mass spectrometry; AlphaScreen, Amplified Luminescence Proximity Homogenous Assay Screen; HADCi, histone deacetylase inhibitor; LMW, low molecular weight; RMSD, root mean-square deviation.

Abstract

The EED (embryonic ectoderm development) subunit of the Polycomb repressive complex 2 (PRC2) plays an important role in the feed forward regulation of the PRC2 enzymatic activity. We recently identified a new class of allosteric PRC2 inhibitors that bind to the H3K27me3 pocket of EED. Multiple assays were developed and used to identify and characterize this type of PRC2 inhibitors. One of them is a genetically encoded EED biosensor based on the EED[G255D] mutant and the split firefly luciferase. This EED biosensor can detect the compound binding in the transfected cells and in the *in vitro* biochemical assays. Compared to other commonly used cellular assays, the EED biosensor assay has the advantage of shorter compound incubation with cells. The *in vitro* EED biosensor is much more sensitive than other label-free biophysical assays (e.g. DSF, ITC). Based on the crystal structure, the DSF data as well as the biosensor assay data, it's most likely that compound-induced increase in the luciferase activity of the EED[G255D] biosensor results from the decreased non-productive interactions between the EED subdomain and other subdomains within the biosensor construct.. This new insight of the mechanism might help to broaden the use of the split luciferase based biosensors.

Key words: PRC2, EED, H3K27me3-pocket, split luciferase, biosensor, EED[G255D]

1. Introduction

Polycomb repressive complex 2 (PRC2) is a methyltransferase complex that can specifically methylate lysine 27 of histone H3. It plays a key role in the epigenetic regulation of gene expression. At least three subunits are required for the enzymatic activity of PRC2: EzH2 (Enhancer of zeste homolog 2), EED (embryonic ectoderm development) and Suz12 (suppressor of zeste 12) [1-5]. EzH2 is the catalytic subunit of PRC2 which contains the binding sites for the cofactor SAM. EED contains a binding site for tri-methylated lysine 27 (H3K27me3), the product of the PRC2 reaction. Binding of H3K27me3 to EED stimulates the catalytic activity of the PRC2 complex through an allosteric mechanism [6, 7]. Thus EED mediates the feed forward regulation of PRC2. In cells, binding of EED to an H3K27me3-bearing nucleosome could also bring the PRC2 complex to its substrate and facilitate the subsequent methylation of the adjacent H3K27me0/1/2-bearing nucleosome.

Recently, we disclosed a novel class of allosteric PRC2 inhibitors that bind to the H3K27me3 pocket of EED [8,9]. We refer this class of inhibitors in this paper as EEDi. Binding of EEDi competitively inhibited the binding of H3K27me3 peptide, thus blocked the H3K27me3-mediated stimulation of PRC2 activity. Surprisingly, EEDi also inhibit the basal enzymatic activity of PRC2 measured in the absence of any stimulatory peptide. The exact mechanism for this allosteric effect is not fully understood as the complex structure of EEDi with the PRC2 complex is not available. In the co-structure of EEDi with EED, binding of EEDi causes significant change in the positions of the three aromatic residues (F97, Y148 and Y365) while the conformational change outside the aromatic cage is subtle. Yet it might be significant enough to affect the intricate interaction of EED with the stimulation responsive motif (SRM) of EzH2 [10-12]; thus prevents PRC2 from adapting the catalytically active conformation.

Several cell-based assays have been developed for characterizing PRC2 inhibitors. The H3K27me3 ELISA assay is the one being used extensively to support the SAR effort. It's a proximal assay that directly read out the consequence of PRC2 inhibition [8]. However, like other histone markers, the apparent half-life for H3K27me3 in cells is very long. It often takes about 48 to 72 hr compound incubation to see any significant change in the H3K27me3 level. The prolonged incubation time makes this assay inadequate for charactering early stage compounds that are usually not potent enough and often have off-target toxicity issues.

To overcome this drawback associated with the H3K27me3 ELISA assay, we evaluated the feasibility of using the split firefly luciferase based biosensor approach to characterize EEDi. Split-luciferase complementation technologies have been widely used to study protein-protein interactions and protein-ligand interactions [13-17]. The underlying mechanism for most of the published split luciferase biosensors is compound-induced large conformational change. For example, in the "kinase activity sensors" [17], a substrate peptide motif and a phospho-S/T/Y binding motif are inserted in the middle of the luciferase. Once phosphorylated, the substrate peptide will "bite" back to the phospho-S/T/Y binding motif and thus change the overall conformation of the biosensor. In the "Abl conformational sensor" reported by Zhou [18], the authors took advantage of the large conformational difference between the activated Abl and the inactivated Abl, and inserted the entire Abl sequence (including the CAP, SH2, SH3 and the catalytic domain) directly in the middle of the firefly luciferase. This sensor was able to detect the conformational change of Abl in cells after treatment with the ATP-pocket inhibitors as well as the myristate-pocket inhibitors [18].

In this paper, we report the development and validation of a robust EED biosensor (based on the EED[G255D] mutant) that can be used to characterize EEDi both in cells and *in vitro*. We also

provide data to suggest that compound-induced increase of the luciferase activity of the EED biosensor is likely from the change in the thermal dynamics of the EED motif rather than from compound-induced large conformational change.

2. Materials and Methods

2.1 Protein expression and purification

EED wt (residues 40-441) sensor and EED[G255D] (residues 40-441) mutant sensors were both cloned in a multiple expression host compatible vector of pTriEx-3, with N-terminal domain of the firefly luciferase (N-Luc) and the C-terminal domain of firefly luciferase (C-Luc) flanking at the N- and C- terminal regions of EED protein respectively, and a FLAG tag was inserted between the N-luc and EED protein, and a His8 tag was added just before the stop codon. The EED sensor proteins were expressed in BL21(DE3) and purified first by a His FF(GE) affinity column followed with a Mono S (GE) column, and finally purified with a superdex 200 16/60 (GE) column in 20 mM HEPES (pH 8.0), 50 mM NaCl, 5% Glycerol, 5 mM DTT. EED wt and EED [G255D] proteins used in AlphaScreen, ITC and DSF were expressed and purified as previously described [8].

2.2 Crystallization and structure determination of EED[G255D]-EBD-EED226 complex

Crystals of EED[G255D] in complex with the peptide and compound were obtained by vapor diffusion in sitting drops incubated at 20°C by mixing 0.1 µL of protein solution (8.4 mg/mL) including 0.5 mM EBD peptide (EZH2 residue 40-68, referred as EED-binding domain), and 0.6 mM EED226 compound and 0.1 µL of reservoir solution containing 10% polyethylene glycol (PEG) 6000, 0.1 M Bicine (pH 9.0). Crystals appeared at the second day. Reservoir solution supplemented with 30% glycerol was used as cryo-solution. Crystals were mounted and flash-

frozen in liquid nitrogen. Diffraction data to 2.03 Å resolution were collected at the Shanghai Synchrotron Radiation Facility (SSRF) beamline BL17U1 and processed using HKL2000 [19] .The structure was solved by molecular replacement using Molrep in the CCP4 suite [20] with the previous EED wt structure (PDB entry 5GSA) as a model [8]. The model was built using COOT [21] and refined using Buster [22].The statistics of the structure refinement and the quality of the final model are summarized in **Table 1.**

Table 1 Data collection and statistics for the structure of EED[G255D]-EBD-EED226 complex

	EED[G255D]-EBD-EED226
PDB entry	5WUK
Data collection	
Space Group	P 2_1 2_12_1
Unit Cell Parameters [Å]	53.1, 80.3, 108.4
α, β, γ[°]	90.00 90.00 90.00
Contents of ASU[1]	
Protein Molecules	1 EED[G255D]-EBD
Ligand Molecules	1 EED226
Resolution [Å]	64.52-2.03 (2.14-2.03)[2]
Unique Reflection	30739 (4427)
Completeness [%]	99.9 (99.9)
Redundancy	6.2 (6.4)
R_{merge} [%]	10.9 (47.0)
I/σ(I)	5.0 (1.6)
Refinement	
Resolution [Å]	26.00-2.03 (2.10-2.03)
No. of Reflections	30632 (2976)
Completeness [%]	99.8 (99.9)
R_{work}[%]	16.2 (16.7)
R_{free}[3][%]	19.1 (21.4)
Average B-factor [Å^2] Overall	27.7
rmsd bonds[Å]/angles[°]	0.010/1.04
Ramachandranplot (allowed)	100%

[1]Asymmetric Unit

[2]numbers in parenthesis are for highest resolution shell

[3]test set uses 5.1% data

2.3 PRC2 complex enzymatic activity assay

PRC2 complex (EZH2/EED/SUZ12/AEBP2/RbAP48) enzymatic assays were performed as previously described [8, 9, 23, 24]. The assay employs liquid chromatography mass spectrometry technology using either histone H3(21-44, K27me0) peptide or recombinant mono-nucleosome as substrate. The co-product SAH formation was detected and quantified by LC/MS/MS using SAH-d_4 as an internal standard (IS) control. For enzymatic activity test of PRC2 wt and PRC2 [EED-G255D] mutant complex, the conditions were as following: 30 nM PRC2 wt or PRC2 [EED-G255D], 5 µM SAM, 5 µM H3(21-44, K27me0) peptide, reaction time 2.5 h. For histone H3(21-44, K27me3) stimulation on PRC2 wt or PRC2 [EED-G255D] mutant complex, the assay was performed as following: 40 nM PRC2 wt or PRC2 [EED-G255D], 1 µM SAM, 0.5 µM recombinant mono-nucleosome, various concentration of histone H3(21-44, K27me3) peptide (0-50 µM), reaction time 2 h.

2.4 EED-H3K27me3 AlphaScreen competition binding assay

To assess EED226 or histone peptide H3(21-44, K27me3) binding affinity to EED wt or EED[G255D] mutant, biotinylated H3K27me3 peptide (19-33) displacement was carried out by AlphaScreen assay. The assay was performed under the conditions of 20 nM His-EED wt (or 200 nM His-EED[G255D] mutant) and 10 nM biotinylated H3K27me3 (19-33) peptide in the buffer containing 25 mM HEPES, pH 8, 0.02% Tween-20, 0.5% BSA. After incubation at room temperature for 20 min in the presence of varying concentrations of compound or peptide, freshly prepared AlphaScreen detection beads mix (nickel chelate acceptor beads and streptavidin donor beads) was added to each well with final concentration of 10 µg/mL for both donor and acceptor beads. After incubation in the dark at room temperature for 1 h, plates were read on EnVision (PerkinElmer) using the AlphaScreen setting adapted for optimal signal

detection with a 615 nm filter, after sample excitation at 680 nm. The emission signal at 615 nm was used to quantify compounds inhibition. AlphaScreen signals were normalized based on the reading coming from the positive (DMSO control) and negative controls (no EED control) to give percentage of activities left. The data were then fitted to a dose response equation using the program Helios (Novartis) to get the IC_{50} values. Each compound was counter-screened by using Biotin-miniPEG-His_6 peptide to determine if compounds alone will interfere with the AlphaScreen beads.

2.5 Detection of compound-induced change in luciferase in cells

293T human embryonic kidney fibroblasts were maintained in Dulbecco's modified Eagle's medium (DMEM) with 10% fetal bovine serum (FBS) and 1X penicillin–streptomycin–glutamine (PSQ). On day 0, cells were split into 100-mm Petri cell culture dishes to achieve 50% to 70% confluence. On day 1, expression constructs for EED sensors were mixed with X-tremeGENE HP DNA Transfection Reagent (DNA 10 µg, X-tremeGENE 20 µL) in 1 mL OptiMEM buffer and incubated at room temperature for 20 min. Then the DNA mixture was added dropwise to a dish of 293T cells. On day 2, transfected cells were trypsinized and seeded into a 384-well white TC plate (Greiner 384 plate 781080) at a density of 10,000 cells/well in 30 µL of medium. On day 3, 10 µL of compounds diluted in medium was added to the cells. Luciferase activities of the cells were measured with Bright-Glo after incubation with compounds.

2.6 Detection of compound-induced change in luciferase in vitro

To assess compounds effect against recombinant EED wt or EED[G255D] sensor proteins, compounds were serially diluted 3-fold in DMSO to obtain a total of twelve screening

concentrations. Compounds at each concentration were then transferred by Mosquito into a 384-well ProxiPlate 384 plus plates (Perkin Elmer). Recombinant sensor proteins (30 nM EED wt or 100 nM EED[G255D]) was prepared in the reaction buffer containing 20 mM Tris-HCl, pH 8.0, 0.01% Triton X-100, 0.5 mM DTT, 0.1% BSA and then added to the above pre-dispensed compounds plate. After 30 min incubation at room temperature, Bright-Glo was added to each well. Plates were read on Envision (Perkin Elmer) after 30 min incubation in the dark at room room temperature.

2.7 Western blot analysis

One-half million 293T cells were transiently transfected with indicated sensor construct. After 24 h of transfection, cells were treated with 10 μM EED226, EI1 or DMSO for 24 h. Cells were collected and lysed with SDS lysis buffer (50 mM Tris-HCl, 2% SDS, 10% glycerin) containing protease inhibitor cocktail tablet (Roche). Protein concentration was determined with BCA kit (Thermo Scientific). Equal amounts of protein from each cell lysate were subjected to SDS/PAGE and transferred to PVDF membranes. The following antibodies were used: anti-histone H3 trimethyl Lys-27 (1:2000; rabbit monoclonal, Cell Signaling 9733); anti-FlAG M2 (1:1000; mouse monoclonal, Sigma F3165); anti-tubulin (DM1A) (1:2000; mouse, Cell Signaling 3873). Blots were visualized with enhanced chemiluminescence (ECL) reagents (Amersham).

2.8 EED wt or EED[G255D] Differential Scanning Fluorimetry (DSF) assay

Compound or peptide was freshly prepared in DMSO and added to protein solution of either EED wt or EED[G255D] in DSF buffer (20 mM Tris, pH 8.0, 100 mM NaCl, 5 mM DTT, 10%

glycerol). After 10 min incubation at room temperature, a 1:10 pre-dilution of SYPRO Orange dye (Invitrogen; 5000x) in buffer was added to the protein solution to give a final concentration of 5x of dye. The experiment (10 µL/ reaction) was run in triplicate with Microseal 384-Well PCR Plates (Bio-rad). The final conditions in the experimental well were 5x SYPRO Orange, 100 µM compound or peptide, 5 µM protein and 5% (v/v) DMSO in analysis buffer. Reference wells were also included by replacement of compound or peptide with DMSO. The plates were sealed with optically clear, adhesive seal (Bio-rad), and centrifuge at 2000 g for 2 min. DSF was carried out in a CFX384 Touch™ Real-Time PCR machine (Bio-rad). Temperature was increased by 1 °C/min from 20 to 85 °C after an initial equilibration at 10 °C for 5 minutes. The melt curve data was exported into a text file and accurate T_m values were calculated from a modified Boltzmann equation using an internal program in combination of pipeline pilot and the statistics package R. The reported T_m values are based on the mean values from two independent experiments in triplicates. The standard deviation of T_m was smaller than 0.1 °C from all replicates.

2.9 Isothermal titration calorimetry (ITC)

The ITC binding studies were performed with an Auto-ITC200 instrument from GE Healthcare at 25 °C. All proteins and compounds were prepared in ITC buffer (20 mM Tris-HCl, pH 8.0, and 100 mM NaCl, 5% glycerol, 5 mM DTT, and 0.3% DMSO). EED226 at 150 µM (0.15 mL) was injected into the samples cell containing 15 µM EED wt or EED[G255D] mutant (0.45 mL). Proteins were titrated with EED226 directly with first injection of 0.4 µL then 2 µL injection with a total of 19 injections. The control experiment was performed by titration of EED226 into ITC buffer and then subtracted from each experiment to adjust for the heat of dilution of ligands.

ITC data was analyzed with the ITC-Origin 7.0 software (MicroCal Inc.) based on a "one-site binding" reaction.

3. Results and discussion

3.1 Development of a split luciferase-based EED sensor assay

To develop a proximal cellular assay for PRC2 inhibitors that require shorter incubation time, we first designed several "PRC2 activity sensors" using the split luciferase approach. In these sensors, N-terminal histone H3(1-44) peptide, EED(40-441), the N-terminal domain of the firefly luciferase (N-Luc) and the C-terminal domain of firefly luciferase (C-Luc) were linked together in different combinations (one of the constructs was shown in Fig. 1A). In these constructs, the H3(1-44) peptide motif was designed as the substrate for the endogenous PRC2. EED(40-441) motif was designed as the binder for the tri-methylated lysine 27 on H3(1-44). The design principle for these "PRC2 activity sensors" is similar to the kinase activity sensors [17]. It's expected that, once methylated by the endogenous PRC2, the trimethylated H3K27me3 peptide will bind to EED(40-441), and thus change the conformation of these "PRC2 activity sensors".

Several constructs were evaluated in transiently transfected 293T cells using a SAM-competitive inhibitor EI1 [24] and EED226 (an EEDi) [8,9]. Unfortunately, we were not able to see any change in the luciferase signal after treating the cells with EI1. From western blot, it's apparent that the H3 peptide motif in these "PRC2 activity sensors" cannot be efficiently trimethylated by the endogenous PRC2 in 293T cells (Fig. 1B). Thus, even though EI1 can efficiently suppress the PRC2 activity in the 293T cells as demonstrated by the reduction of H3K27me3 level on the endogenous histone H3 (Fig. 1B), they don't affect the methylation status of H3K27 on the "PRC2 activity sensors". It's likely that these biosensor proteins cannot be incorporated into the

chromatin and thus cannot be efficiently methylated by PRC2. Full-length histone H3 rather than the N-terminal H3 peptide might be needed.

In contrast to EI1, we did observe a small but consistent increase of luciferase signal after EED226 treatment (Fig. 1C), suggesting that binding of EED226 to the EED motif in the "PRC2 activity sensors" might be sufficient to affect the luciferase activity. To confirm this, we removed the H3 peptide from the "PRC2 activity sensors" and generated an "EED-binder sensor" (Fig. 1A). For comparison, we also made a control construct, "EED-luc fusion sensor", in which the EED(40-441) sequence was inserted in front of the intact luciferase. These two constructs were then studied in 293T cells. As shown in Fig. 1D, EED226 significantly increased the luciferase signal of the EED wt sensor after 24 hr treatment. The AC50 for EED226 in the EED wt sensor assay (24 hr) was similar to its IC50 in the H3K27me3 ELISA assay (48 hr) [8]. As expected, the SAM-competitive PRC2 inhibitor EI1 showed little effect on the EED wt sensor (Fig. 1D). Neither EED226 nor EI1 affected the luciferase signal of the non-split EED-Luc fusion construct (data not shown).

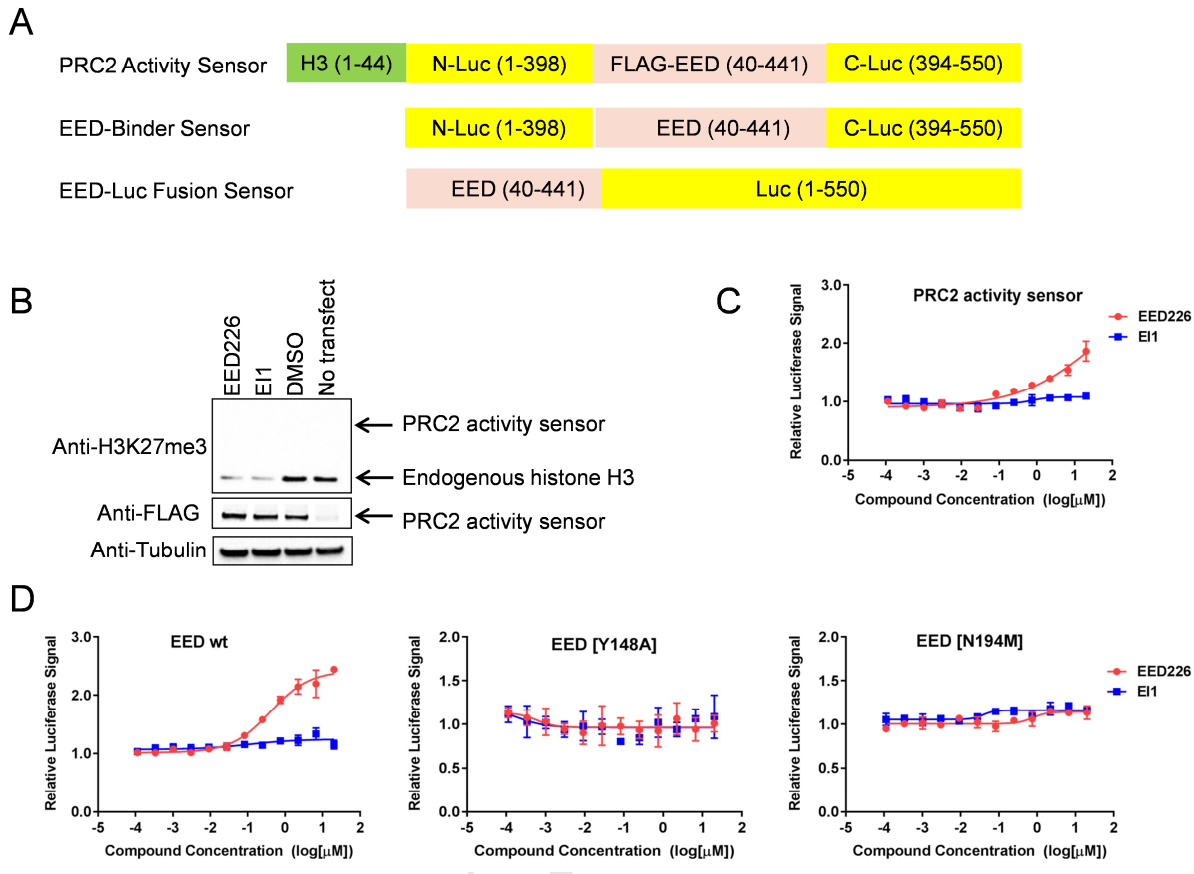

Fig. 1. (A) The domain structure of biosensors. PRC2 activity sensor contains a PRC2 substrate peptide H3 (1-44). EED-binder sensor contains EED (40-441) flanked by the N-terminal [N-Luc] and C-terminal [C-Luc] domain of the firefly luciferase reporter molecule. (B) Western blot analysis of PRC2 activity biosensor in 293T cell. Trimethylation of K27 on the endogenous histone H3 can be detected, which can be reduced by EI1 and EED226 treatment. However, no H3K27me3 was detected on the PRC2 activity biosensor. (C) Concentration-dependent effects of EED226 and EI1 on PRC2 activity sensor in transfected 293T cells. (D) Concentration-dependent effects of EED226 and EI1 on the wt and mutants EED-binder sensors in transfected 293T cells.

To further confirm that the EED226-mediated increase of the luciferase signal is indeed due to the binding of EED226 to the EED wt sensor, several mutant EED sensors were generated and studied. Three aromatic residues: F97, Y148 and Y365 that are critical for the binding of the

EED inhibitors were each mutated to an alanine residue [6-8]. As expected, mutation at each of these three aromatic residues dramatically reduced the AC_{50} for the EED inhibitors in the EED sensor assay (data for EED[Y148A] is shown in Fig. 1D). Another residue that is critical for EEDi binding is N194 which stabilizes EED226 through hydrogen-bond interaction [8]. EED[N194M] mutant sensor abolished the compound-induced luciferase change completely (Fig. 1D).

3.2 Optimization of the EED sensor with EED[G255D] mutant

The EED sensor assay described above is not very robust. To get a higher assay window, overnight incubation is required. This long incubation time makes it prone for interference from toxic compounds or compounds that can affect the expression level of the transgenes, such as histone deacetylase inhibitors (HDACi). To overcome these drawbacks, we then evaluated several EED mutants and found the EED[G255D] looks promising and was chosen for detailed characterization.

3.2.1 EED[G255D] mutation does not significantly affect LMW EEDi binding to EED: The G255D mutation on EED was identified from myeloproliferative neoplasms patients [25]. This mutation (on EED) dramatically reduces the basal (un-stimulated) activity of PRC2 complex (Fig. 2A) [25]. It also dramatically increases the K_{act} (EC50) of the H3K27me3 peptide (Fig. 2B). Consistant with the enzymology data, H3K27me3 peptide showed a much lower apparent affinity for the EED[G255D] mutant in the EED-H3K27me3 binding/competition AlphaScreen assay (Fig. 2C).

Even though the EED[G255D] mutation reduces the binding of H3K27me3 peptide to EED, its effect on the binding of the low molecular weight (LMW) EEDi seems to be less dramatic. As

shown in Fig. 2D, EED226 showed similar IC50 in the EED wt/H3K27me3 and the EED[G255D]/H3K27me3 binding AlphaScreen assays. In ITC (Fig. 2E and 2F), EED226 showed slightly higher affinity for the EED[G255D] mutant, with K_D value of 30 nM and 14 nM for EED wt and EED[G255D] mutant respectively.

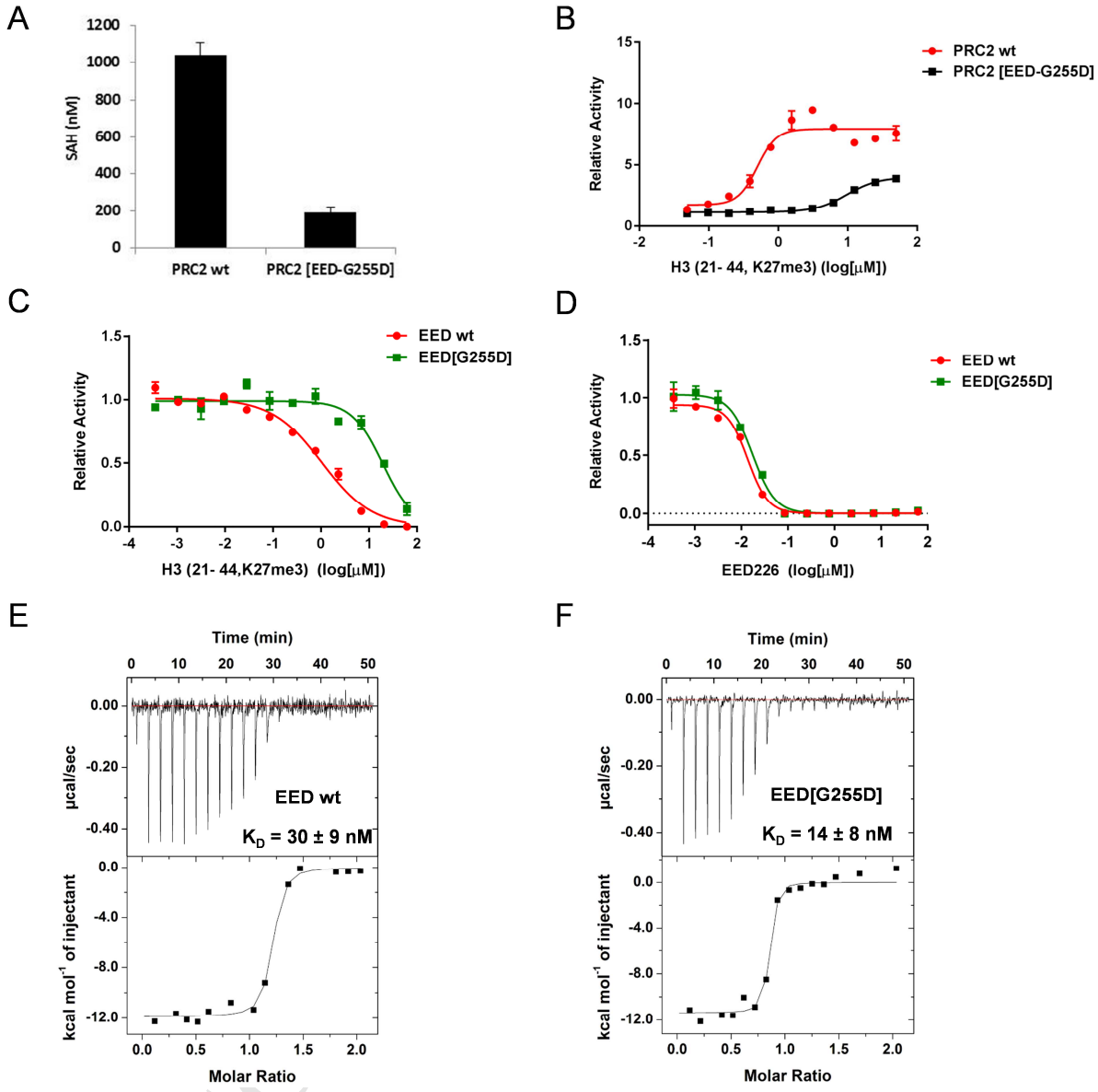

Fig. 2. (A) PRC2 complex bearing EED[G255D] mutation showed reduced enzymatic activity against H3(21-44, K27me0) peptide substrate. (B) Stimulation of PRC2 complex activity by H3(21-44, K27me3) peptide in the enzymatic assay with mono-nucleosome particle as substrate. K_{act} is defined as the concentration of H3(21-44, K27me3) peptide where the stimulation is half-maximum. (C) Untagged H3(21-44, K27me3) peptide showed reduced potency in EED[G255D]-H3K27me3 AlphaScreen binding assay. (D) EED226 potency is unchanged in

EED[G255D]-H3K27me3 AlphaScreen binding assay. (E) Isothermal titration calorimetry (ITC) for EED226 binding to EED wt. (F) Isothermal titration calorimetry (ITC) for EED226 binding to EED[G255D] mutant.

***3.2.2 EEDi increase the luciferase signal of EED[G255D] biosensor with a faster kinetics*:** As the EED[G255D] mutant does not significantly affect the potency of the EED binders, we then generated an EEDi sensor based on it. As expected, all active EED binders (EED226, EED014, EED600 and EED162) [26] increased the luciferase signal of EED[G255D] biosensor after overnight incubation (data not shown). Interestingly, we also observed a dramatic increase of signal after only 10 min or 60 min treatment (Fig. 3A and 3B). In contrast, there is no signal increase observed for a SAM-competitive inhibitor EI1 and EED381, an inactive EED226 analog [8]. For such short incubation time, no significant signal increase was observed for the EED wt sensor after compounds treatment (Fig. 3C and 3D). Similarly, HDACi SAHA did not affect the luciferase signal for either the EED wt sensor or the EED[G255D] mutant sensor after 10 or 60 min incubation (Fig. 3), while overnight incubation of SAHA increases the luciferase signal for both sensors (Data not shown). As expected, 60 min treatment of cells with EED226 or SAHA did not affect the protein level of the EED sensors on Western blot (data not shown).

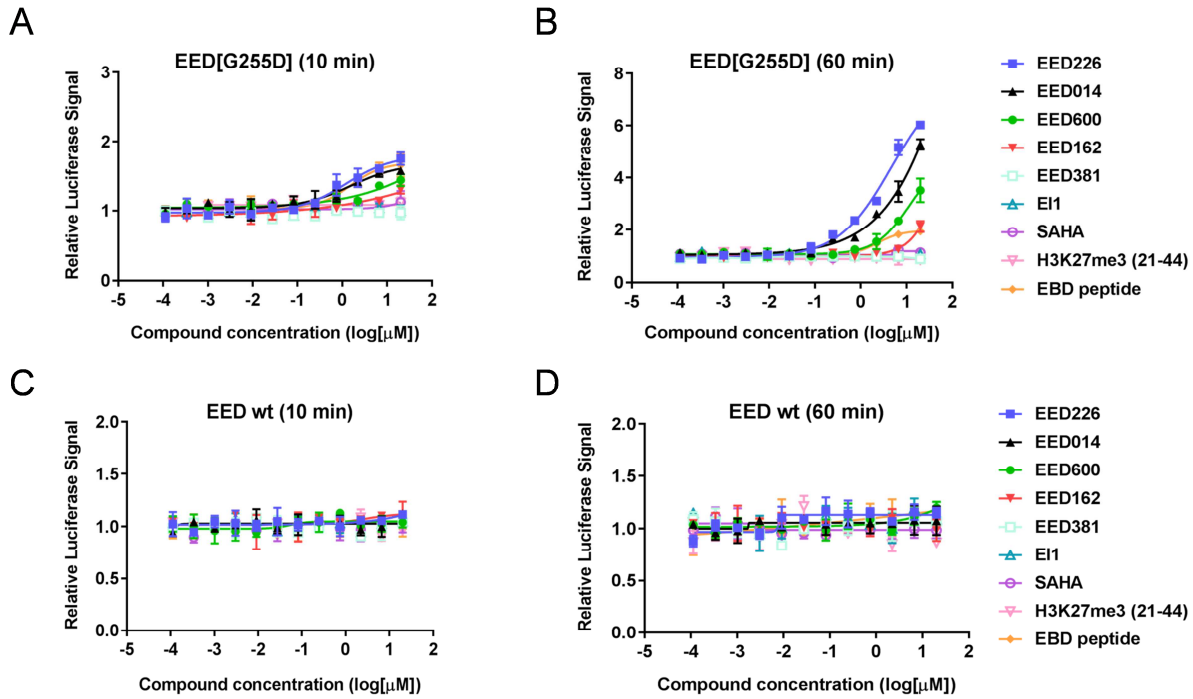

Fig. 3. Compounds induced luciferase signal increase in cells after (A) 10 min incubation in EED[G255D] sensor assay; (B) 60 min incubation in EED[G255D] sensor assay; (C) 10 min incubation in EED wt sensor assay; (D) 60 min incubation in EED wt sensor assay.

3.2.3 Evaluation of the recombinant N-Luc-EED[G255D]-C-Luc protein in vitro: The fast kinetics of EEDi compounds on the EED[G255D] sensor in the cellular assay and the lack of effect on the protein level on the Western blot strongly suggested that the EEDi might directly affect the specific activity of the mutant sensor. To confirm this, we expressed and purified both the EED wt sensor and the mutant EED[G255D] sensor protein and evaluated them *in vitro*. As shown in Fig. 4, all four active EED binders increased the luciferase signal of the recombinant EED[G255D] mutant sensor, while it showed no effect on the recombinant EED wt sensor

protein. In addition, the EBD peptide (EZH2 residue 40-68, referred as EED-binding domain) also increased the luciferase signal of the mutant sensor protein, whereas the H3K27me3 peptide (up to 100 µM) showed no effect. Moreover, the same rank order of potency was observed between cellular and *in vitro* sensor assays for all LMW EED binders except EBD peptide. The weaker effect of EBD peptide in cellular assay is most likely due to its low permeability.

Taken together, our data showed that the EED[G255D] mutant sensor can clearly "sense" the binding of a compound to it. The increased luciferase activity after compound binding does not require the "help" of any additional protein. It is worth to note that the basal luciferase activity for the G255D mutant sensor is only ca. 20% of that the EED wt sensor in the absence of any compound. Nevertheless, this biosensor assay based on the EED[G255D] is still extremely sensitive. Nanomolar concentration of the G255D mutant sensor protein is sufficient to give a robust signal window for the EEDi compounds and the EBD peptide.

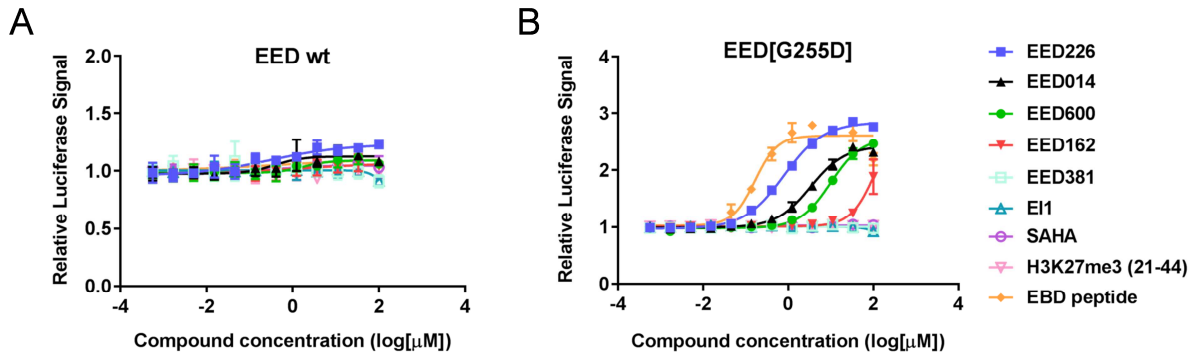

Fig. 4. Compounds-induced luciferase signal change *in vitro* for the (A) recombinant EED wt sensor protein; and (B) the recombinant EED[G255D] sensor protein. Compounds or peptides were incubated with recombinant sensor proteins for 30 min before detection. 100 nM of the recombinant EED[G255D] sensor protein and 30 nM of the recombinant EED wt sensor proteins were used.

3.3 Potential mechanism of the EED sensor

Large conformational change is the underlying mechanism for most of the firefly luciferase based biosensor. To understand the mechanism for the EED[G255D] mutant sensor, we solved the structure of the EED[G255D] mutant complexed with EED226 and EBD (Fig. 5) and compared it with the published **wtEED:EED226:EBD** structure [8]. Overall, the two structures are very similar with root mean-square deviation (RMSD) of 0.221 Å for the 335 pairs of Cα atoms (Fig. 5A). The N-terminal and C-terminal ends are aligned very well between these two EED structures. It's worth to mention that the N-terminal residue (K76) and the C-terminal residue (R441) of the EED[G255D] visible in the x-ray structure is very close to each other (with distance of ca. 17.7 A); and they are on the same side of the EED disk (Fig. 5B). Therefore, they should be able to interact with each other "freely" to form a "productive" conformation (conformation 1 in Fig. 6). In addition, there are also 36 amino acid residues N-terminal to K76 that were included in the EED biosensor constructs; this could add additional flexibility to the EED biosensor.

The most obvious differences between the **EED[G255D]:EED226:EBD** and the **wtEED:EED226:EBD** structures are at the side chains of the Try308 and Trp364 residues (Fig. 5). In the **EED[G255D]:EED226:EBD** structure, Trp364 is more exposed while Try308 is more buried. These small localized conformational differences could alter the nonspecific interaction between the EED propeller domain and the other domains/motifs within the EED biosensors (e.g. the N-Luc, the C-luc domains and/or the linker sequences). This in turn could change the fraction of the "active" EED biosensor and the overall luciferase signal. As the EED[G255D] mutant sensor has a lower luciferase activity, thus it's possible that the G255D mutation

increases these non-specific interaction and decreased the fraction of the active/productive conformations of the EED biosensor (Fig. 6).

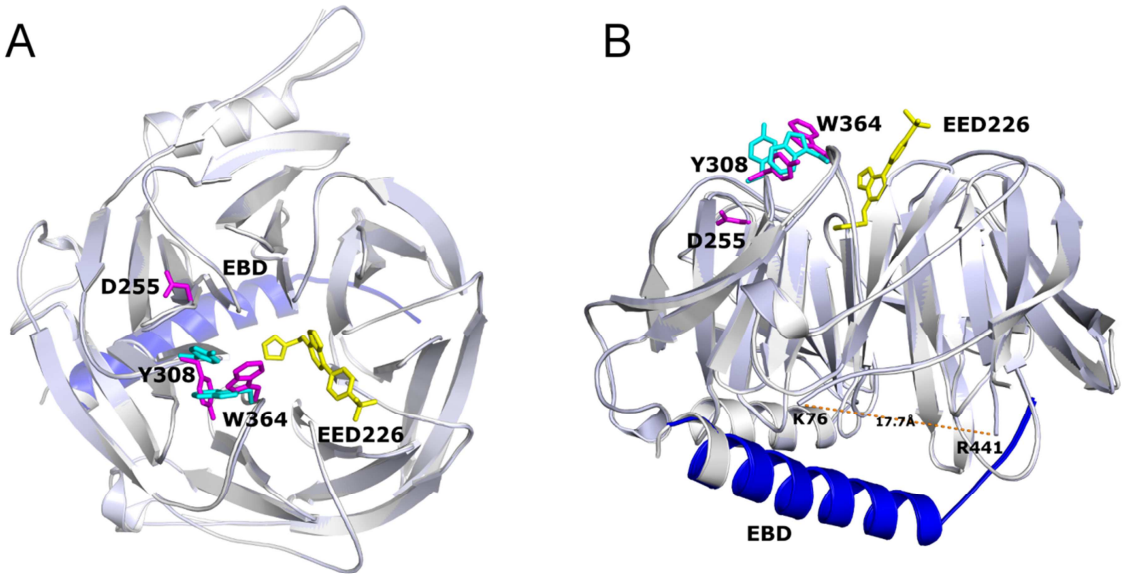

Fig. 5. Comparison of structures between EED[G255D] and wt EED in complex with EBD and EED226. (A) Overall structures of EED [G255D]-EBD-EED226 complex (in light blue color) aligned with wt EED-EBD-EED226 complex (in gray color, PDB code 5GSA) [8]. EED226 compound in yellow stick model binds to the top center of the β-propeller formed by seven WD40 units of EED. EBD peptide (in blue color) binds to the bottom side of the β-propeller structure. D255, W364 and Y308 residues in EED [G255D] molecule are colored in magenta while Y308 and W364 residues in wt EED molecule are colored in cyan. (B) Side view of structures shown in (A). The distance between the N-terminal residue (K76) and the C-terminal residue (R441) of the EED [G255D] was shown as orange dashed line.

The G255D mutation also decreased the thermal stability of the EED protein in the DSF assay. As shown in Table 2, the EED[G255D] mutant protein has a T_m of 45.1 ^oC, while the EED wt protein has a T_m of 52.5 ^oC. Binding of EED226 and the EBD peptide significantly stabilized both the EED wt (ΔT_m is 8.5 ^oC and 6.2 ^oC, respectively) and the EED[G255D] mutant proteins (ΔT_m is 11.1 ^oC and 9.1 ^oC, respectively). In comparison, binding of the H3K27me3 peptide, even though to the same pocket as that for EED226, showed no effect. Thus, the behaviors of the LMW compounds and the peptides in the EED[G255D] DSF assay are the same as that in the EED[G255D] biosensor assay, suggesting the underlying mechanisms for these two assays are similar. Compared to the DSF assay, the EED biosensor assay is much more sensitive and it requires much less protein (nM vs μM in the DSF assay).

Table 2 Ligand binding to EED wt and EED[G255D] mutant detected by DSF[a]

	EED wt		**EED [G255D]**	
	T_m (^{o}**C**)	ΔT_m (^{o}**C**)	T_m (^{o}**C**)	ΔT_m (^{o}**C**)
APO	52.5		45.1	
EED226	61.0	8.5	56.2	11.1
EBD	58.7	6.2	54.2	9.1
H3K27me3	52.5	0	45.9	0.8

[a] The reported T_m values are based on the mean values from two independent experiments in triplicates. The standard deviation of T_m was smaller than 0.1 °C from all replicates.

Taken together, we proposed the following mechanism to explain the EEDi induced increase in the luciferase activity for the EED[G255D] biosensor (see Fig. 6). The G255D mutation destabilizes EED and increases the non-productive interaction of the EED propeller domain with the N-luc, C-luc or the linker sequences. This in turn decreased the faction of the productive conformation and thus the basal luciferase activity for the EED[G255D] biosensor. Binding of EEDi stabilizes and rigidifies the EED[G255D] mutant. This in turn reduced the fraction of the non-productive conformation and increased the fraction of the "active" conformation, and thus the overall luciferase activity. In comparison, the non-productive interaction between different domains within the EED wt biosensor is low, and thus the EED wt sensor has a higher basal luciferase activity. Binding of EEDi compounds to the EED wt sensor do not further increase the fraction of the productive conformation.

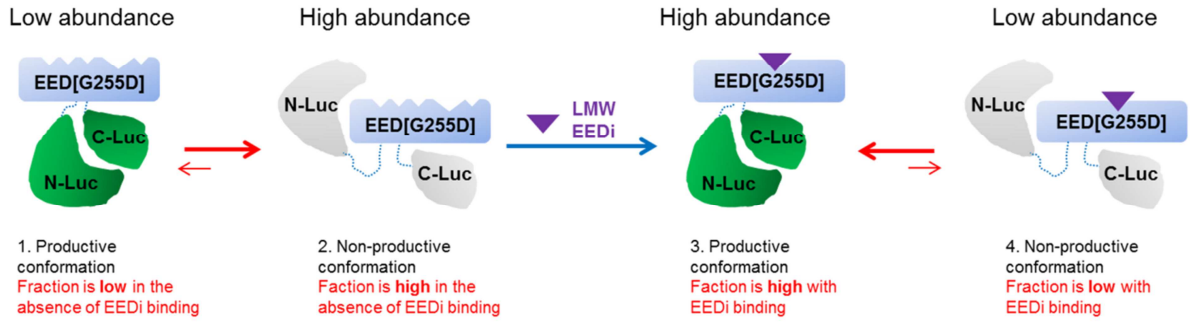

Fig. 6. The proposed mechanism for the EED[G255D] biosensor. The EED[G255D] biosensor can adapt multiple conformations, some have high luciferase activities (e.g. the #1 productive conformation) while others have low or no luciferase activities (e. g. the #2 non-productive conformation). In the absence of a LMW binder, a larger fraction of the EED[G255D] sensor might adapt the non-productive conformations as compared to the EED wt biosensor (due to the increased non-specific interaction of N-Luc and/or C-Luc with the EED[G255D] motif). This can explain why the EED[G255D] sensor has lower basal activity as compared to the EED wt sensor. Binding of LMW EED binders to H3K27me3 pocket on EED stabilizes the EED[G255D], which lead to a significant reduction

of the non-specific interaction between the N-Luc and/or C-Luc and the EED[G255D] motif. This in turn increases the faction of the productive conformation (#3) and thus the luciferase signal.

4. Conclusions:

Using the split luciferase approach, we have developed a robust EED sensor assay with the EED[G255D] mutant. This sensor can detect the compound-induced luciferase signal change in both cellular context and in the *in vitro* biochemical assay. More importantly, the new underlying mechanism could potentially be used to guide the design of other firefly luciferase-based biosensors.

Acknowledgements

This work was supported by China Novartis Institutes for Biomedical Research. We would like to thank Ying Lin, Zhaofu Wang and Zhenting Gao for the helpful discussions.

Accession codes

The atomic coordinates and structure factors for the EED226 compound bound EED[G255D] co-crystal structures (accession codes 5WUK) has been deposited in the Protein Data Bank, Research Collaboratory for Structural Bioinformatics, Rutgers University, New Brunswick, NJ (http://www.rcsb.org)

References

[1] R. Cao, L. Wang, H. Wang, L. Xia, H. Erdjument-Bromage, P. Tempst, R.S. Jones, Y. Zhang, Role of histone H3 lysine 27 methylation in Polycomb-group silencing, Science, 298 (2002) 1039-1043.

[2] R. Margueron, D. Reinberg, The Polycomb complex PRC2 and its mark in life, Nature, 469 (2011) 343-349.

[3] L. Morey, K. Helin, Polycomb group protein-mediated repression of transcription, Trends in biochemical sciences, 35 (2010) 323-332.

[4] M.M. O'Meara, J.A. Simon, Inner workings and regulatory inputs that control Polycomb repressive complex 2, Chromosoma, 121 (2012) 221-234.

[5] J.A. Simon, C.A. Lange, Roles of the EZH2 histone methyltransferase in cancer epigenetics, Mutation research, 647 (2008) 21-29.

[6] R. Margueron, N. Justin, K. Ohno, M.L. Sharpe, J. Son, W.J. Drury, 3rd, P. Voigt, S.R. Martin, W.R. Taylor, V. De Marco, V. Pirrotta, D. Reinberg, S.J. Gamblin, Role of the polycomb protein EED in the propagation of repressive histone marks, Nature, 461 (2009) 762-767.

[7] C. Xu, C. Bian, W. Yang, M. Galka, H. Ouyang, C. Chen, W. Qiu, H. Liu, A.E. Jones, F. MacKenzie, P. Pan, S.S. Li, H. Wang, J. Min, Binding of different histone marks differentially regulates the activity and specificity of polycomb repressive complex 2 (PRC2), Proceedings of the National Academy of Sciences of the United States of America, 107 (2010) 19266-19271.

[8] W. Qi, K. H. Zhao, J. Gu, Y. Huang, Y. Z. Wang, H. L. Zhang, M. Zhang, J. Zhang, Z. T. Yu, L. Li, L. Ten, S. Chuai, C. Zhang, M. X. Zhao, Z. J. Chen, D. Fang, Q. Fei, L. Y. Feng, L. J. Feng, Y. Gao, H. Ge, X. J. Ge, G. B. Li, A. Linger, Y. Lin, Y. Q. Liu, F. J. Luo, M. L. Shi, L. Wang, Z. F. Wang, Y. Y. Yu, J. Zeng, C. H. Zeng, S. L. Zhou, L. J. Zhang, C. Oyang, P. Atadja,

E. Li. An allosteric PRC2 inhibitor targeting EED H3K27me3 binding pocket. Nature Chemical biology.In press.

[9] L. Li, H. Zhang, M. Zhang, M. Zhao, L. Feng, X. Luo, Z. Gao, Y. Huang, O. Ardayfio, J.H. Zhang, Y. Lin, H. Fan, Y. Mi, G. Li, L. Liu, L. Feng, F. Luo, L. Teng, W. Qi, J. Ottl, A. Lingel, D.E. Bussiere, Z. Yu, P. Atadja, C. Lu, E. Li, J. Gu, K. Zhao, Discovery and Molecular Basis of a Diverse Set of Polycomb Repressive Complex 2 Inhibitors Recognition by EED, PloS One, 2017 Jan 10;12(1):e0169855. doi: 10.1371/journal.pone.0169855.

[10] A. Brooun, K.S. Gajiwala, Y.L. Deng, W. Liu, B. Bolanos, P. Bingham, Y.A. He, W. Diehl, N. Grable, P.P. Kung, S. Sutton, K.A. Maegley, X. Yu, A.E. Stewart, Polycomb repressive complex 2 structure with inhibitor reveals a mechanism of activation and drug resistance, Nat Commun, 7 (2016) 11384.

[11] L. Jiao, X. Liu, Structural basis of histone H3K27 trimethylation by an active polycomb repressive complex 2, Science, 350 (2015) aac4383.

[12] N. Justin, Y. Zhang, C. Tarricone, S.R. Martin, S. Chen, E. Underwood, V. De Marco, L.F. Haire, P.A. Walker, D. Reinberg, J.R. Wilson, S.J. Gamblin, Structural basis of oncogenic histone H3K27M inhibition of human polycomb repressive complex 2, Nat Commun, 7 (2016) 11316.

[13] K.E. Luker, M.C. Smith, G.D. Luker, S.T. Gammon, H. Piwnica-Worms, D. Piwnica-Worms, Kinetics of regulated protein-protein interactions revealed with firefly luciferase complementation imaging in cells and living animals, Proceedings of the National Academy of Sciences of the United States of America, 101 (2004) 12288-12293.

[14] H. Mano, M. Nishikawa, K. Yasuda, S. Ikushiro, N. Saito, M. Takano, A. Kittaka, T. Sakaki, Development of Novel Bioluminescent Sensor to Detect and Discriminate between Vitamin D Receptor Agonists and Antagonists in Living Cells, Bioconjug Chem, 26 (2015) 2038-2045.

[15] T. Ozawa, A. Kaihara, M. Sato, K. Tachihara, Y. Umezawa, Split luciferase as an optical probe for detecting protein-protein interactions in mammalian cells based on protein splicing, Analytical chemistry, 73 (2001) 2516-2521.

[16] V. Villalobos, S. Naik, D. Piwnica-Worms, Current state of imaging protein-protein interactions in vivo with genetically encoded reporters, Annual review of biomedical engineering, 9 (2007) 321-349.

[17] L. Zhang, K.C. Lee, M.S. Bhojani, A.P. Khan, A. Shilman, E.C. Holland, B.D. Ross, A. Rehemtulla, Molecular imaging of Akt kinase activity, Nature medicine, 13 (2007) 1114-1119.

[18] V. Zhou, X. Gao, S. Han, A. Brinker, J.S. Caldwell, X.J. Gu, An intracellular conformational sensor assay for Abl T315I, Analytical biochemistry, 385 (2009) 300-308.

[19] Z. Otwinowski, W. Minor, [20] Processing of X-ray diffraction data collected in oscillation mode, Methods Enzymol, 276 (1997) 307-326.

[20] A. Vagin, A. Teplyakov, Molecular replacement with MOLREP, Acta Crystallogr D Biol Crystallogr, 66 (2010) 22-25.

[21] P. Emsley, K. Cowtan, Coot: model-building tools for molecular graphics, Acta Crystallogr D Biol Crystallogr, 60 (2004) 2126-2132.

[22] E. Blanc, P. Roversi, C. Vonrhein, C. Flensburg, S.M. Lea, G. Bricogne, Refinement of severely incomplete structures with maximum likelihood in BUSTER-TNT, Acta Crystallogr D Biol Crystallogr, 60 (2004) 2210-2221.

[23] S. Li, X.J. Gu, Q. Hao, H. Fan, L. Li, S. Zhou, K. Zhao, H.M. Chan, Y.K. Wang, A liquid chromatography/mass spectrometry-based generic detection method for biochemical assay and hit discovery of histone methyltransferases, Analytical biochemistry, 443 (2013) 214-221.

[24] W. Qi, H. Chan, L. Teng, L. Li, S. Chuai, R. Zhang, J. Zeng, M. Li, H. Fan, Y. Lin, J. Gu, O. Ardayfio, J.H. Zhang, X. Yan, J. Fang, Y. Mi, M. Zhang, T. Zhou, G. Feng, Z. Chen, G. Li, T. Yang, K. Zhao, X. Liu, Z. Yu, C.X. Lu, P. Atadja, E. Li, Selective inhibition of Ezh2 by a small molecule inhibitor blocks tumor cells proliferation, Proceedings of the National Academy of Sciences of the United States of America, 109 (2012) 21360-21365.

[25] J. Score, C. Hidalgo-Curtis, A.V. Jones, N. Winkelmann, A. Skinner, D. Ward, K. Zoi, T. Ernst, F. Stegelmann, K. Dohner, A. Chase, N.C. Cross, Inactivation of polycomb repressive complex 2 components in myeloproliferative and myelodysplastic/myeloproliferative neoplasms, Blood, 119 (2012) 1208-1213.

[26] Huang Y, Zhang J, Yu Z, Zhang H, Wang Y, Lingel A, Qi W, Gu J, Zhao K, Shultz MD, Wang L, Fu X, Sun Y, Zhang Q, Jiang X, Zhang J, Zhang C, Li L, Zeng J, Feng L, Zhang C, Liu Y, Zhang M, Zhang L, Zhao M, Gao Z, Liu X, Fang D, Guo H, Mi Y, , Gabriel T DM, Atadja P, Oyang C. Discovery of first-in-class, potent and orally bioavailable EED inhibitors with robust anti-cancer efficacy. J Med Chem. 2016, under review.